Interference and crosstalk in double optical tweezers using a single laser source

Pierre Mangeol and Ulrich Bockelmann[a]
*Laboratoire de Nanobiophysique, UMR CNRS Gulliver 7083, ESPCI, 10 Rue Vauquelin,
75005 Paris, France*

Experimental studies of single molecule mechanics require high force sensitivity and low drift, which can be achieved with optical tweezers. We built an optical tweezer setup for force measurements in a two bead assay. A cw infrared laser beam is split by polarization and focused by a high numerical aperture objective to create two traps. The same laser is used to form both traps and to measure the force by back focal plane interferometry. We show that although the two beams entering the microscope are designed to exhibit orthogonal polarization, interference and a significant parasitic force signal occur. Comparing the experimental results with a ray optics model, we show that the interference patterns are caused by the rotation of polarization on microscope lens surfaces and slides. The model qualitatively describes the pattern and the dependence of the parasitic force signal on the experimental parameters. We present two different approaches to experimentally reduce the crosstalk, namely, polarization rectification and frequency shifting. © *2008 American Institute of Physics.* [DOI: 10.1063/1.2957652]

I. INTRODUCTION

Optical tweezers have been used over the two past decades to probe biological objects of various sizes, from whole cells down to individual proteins. Force measurement devices based on double optical tweezers have initially been used to manipulate nonspherical particles such as bacteria,[1] and have increasingly become important tools for single molecule studies of nucleic acids,[2,3] and their interactions with proteins.[4,5]

An important feature of double optical tweezers derived from a single laser source is that although the absolute position of each trap is sensitive to external mechanical perturbations, their relative position can be precisely imposed. Beam steering may be achieved with galvanometer, piezoelectric tilt mount,[3,6] or acousto-optic deflectors.[4] The force acting on one bead is often measured with the back focal plane method,[7] which allows us to decouple the force signal from trap displacement and, hence, external vibrations. The two traps usually exhibit perpendicular polarization in order to reduce interference as well as to easily discriminate between them for detection. A laser of a different wavelength can be used for detection, but a parasitic signal may then arise from the relative drift between the trapping and detection lasers.

When one of the two trapping beams is used for force measurement, it has to be distinguishable from the second beam of the double trap. Orthogonal polarizations can be used for this purpose. However, when linearly polarized light goes through a system of microscope objectives, such as in an optical tweezers apparatus, it suffers from the rotation of polarization,[8,9] resulting in a nonhomogeneous polarization when it exits the microscope. Consequently, important crosstalk may occur when force is measured in this configuration.

In this article we first consider the rotation of polarization for a Gaussian beam in a simple model. Crosstalk coming from the rotation of polarization is evaluated, and we use the theoretical results to describe the interference patterns experimentally observed in the back focal plane method. Finally, we consider two different approaches to significantly reduce the crosstalk.

II. ROTATION OF POLARIZATION IN A MICROSCOPE

Conventional polarizing microscopy suffers from the rotation of polarization on lens surfaces or slides, which results in a loss of contrast when imaging a sample.[8,9] A simple explanation of the rotation of polarization can be given as follows. For a linearly polarized beam refracting on the surface of a lens, the electric field exhibits different parallel and perpendicular components relative to the plane of incidence, depending on the position on the lens. Since, according to the Fresnel equations, the two components are refracted differently, the polarization of the total electric field is rotated. As described in more detail in the following sections, this effect induces difficulties when detecting force with double optical tweezers.

We theoretically describe the propagation of light in a simple model to give a qualitative understanding of the effects coming from the rotation of polarization in optical tweezers. These effects are of general validity for centered systems, and the main results regarding field symmetry are the same for complex objectives. In our description, the trapping objective and the condenser collecting light from a trapped particle are modeled by two planoconvex lenses, faced front to front (as presented in Fig. 5). We assume a

---

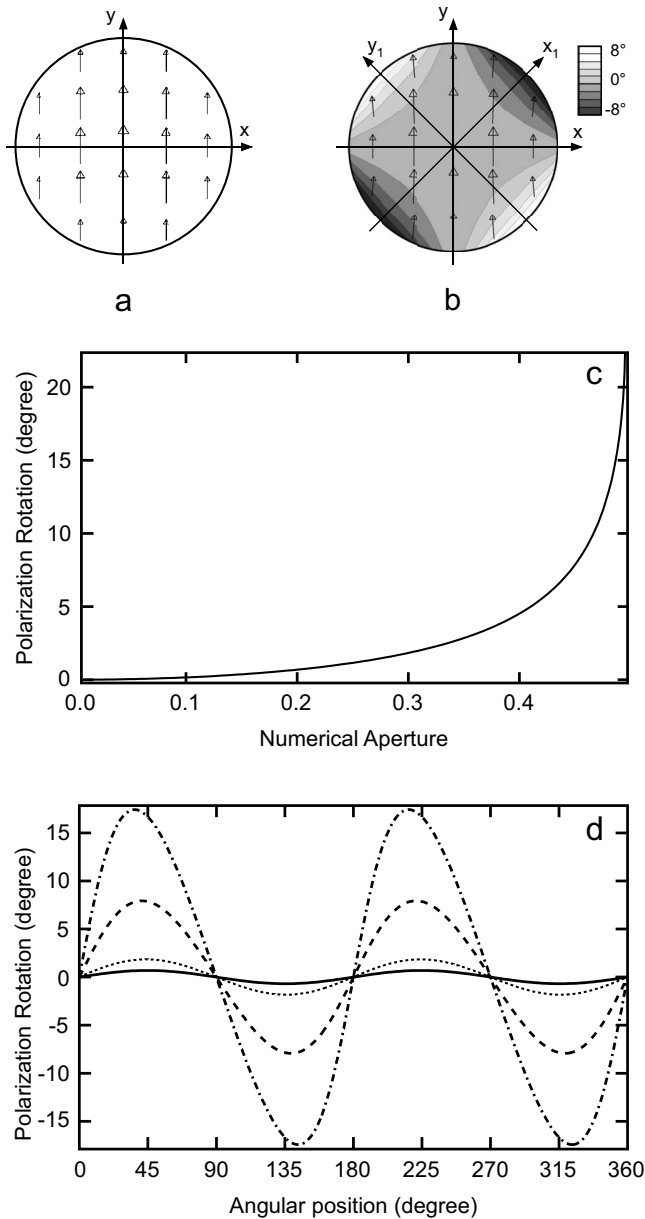[a]Electronic mail: ulrich.bockelmann@espci.fr.

FIG. 1. Rotation of polarization of a Gaussian beam $E = E_0 e^{-r^2/r_L^2}$ passing the two lens system. The electric fields are limited to a 3.8 mm disk. (a) Incident electric field. (b) Calculated transmitted electric field in the back focal plane of the second lens. The lines of the contour plot correspond to the rotation of polarization of $-8°$, $-6°$, $-4°$, $-2°$, $2°$, $4°$, $6°$, and $8°$, and gray scales are used to facilitate visualization. The x_1 and y_1 axes are the first and second bisecting lines. The rotation of polarization of the electric field exiting from the two lens system (c) on the y_1 axis for $y_1 > 0$ and (d) on the perimeter of NA=0.20 (solid), NA=0.30 (dotted), NA=0.45 (dashed), and NA=0.49 (dash-dotted).

radius r_L of the two planoconvex lenses of 2 mm and a glass refractive index of 1.57. The two lenses are identical, centered on the same axis, and the back focal plane of the first lens coincides with the front focal plane of the second lens. The Gaussian beam entering this two lens system is supposed to be parallel, linearly polarized [Fig. 1(a)] and refracting according to the Fresnel equations. Propagation of light is described in the limit of ray optics, and spherical aberration is neglected.

The electric field occurring in the back focal plane of the second lens is presented in Fig. 1(b). Polarization is rotated,
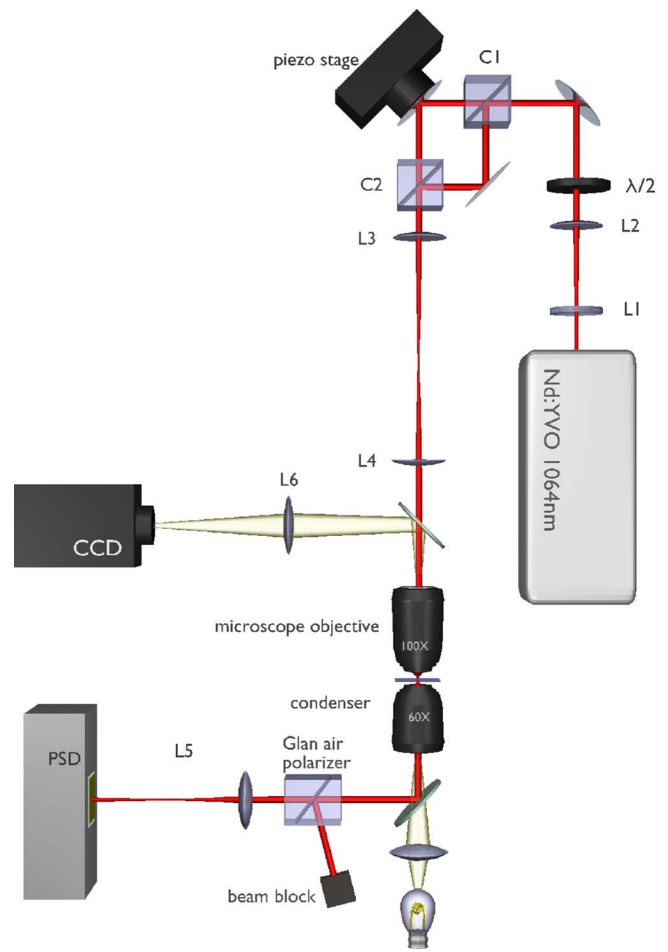

FIG. 2. (Color online) Schematic layout of the double optical tweezers setup. Light pathways are indicated for the laser (red), and for the white light used for Köhler illumination and imaging of the sample (yellow).

except for the x and y axes, which are perpendicular to the optical axis and respectively perpendicular and collinear to the incident polarization. For a given direction in the back focal plane starting from the center, the magnitude of the rotation of polarization increases with numerical aperture (NA) [Fig. 1(c)]. For a given radius, the rotation is stronger when the electric field exhibits similar parallel and orthogonal components according to the incidence plane on the lenses. As described in Ref. 10, maximum values are reached close to the x_1 and y_1 axes, but not exactly on these axes, depending on the NA [Fig. 1(d)].

III. EXPERIMENTAL SETUP

Our setup is based on a custom-designed inverted microscope (Fig. 2). Optical components are from Thorlabs (Thorlabs Inc., Newton, NJ) and Lambda (Lambda Research Optics Inc., Costa Mesa, CA). They are mounted on an optical table (Newport Corp., Irvine, CA) for vibration isolation. For optical trapping and force detection, we use a cw linearly polarized diode pumped Nd:YVO$_4$ laser (1.064 μm, 10 W, Millenia IR, Spectra-Physics, Mountain View, CA). To create two independent traps, the laser beam is split by polarization by the combination of a half-wave plate ($\lambda/2$) and a polarizing cube beam splitter (C1). The direction of one of the two

beams is varied by a piezoelectric mirror mount with an integrated position sensor operating in a feedback loop (Mad City Labs Inc., Madison, WI). After recombination with the second polarizing cube beam splitter (C2), the two beams exhibit perpendicular polarization, and their directions are slightly tilted to obtain two separate traps. Lenses (L3) and (L4) image the center of the mirror mounted on the piezoelectric stage on the back focal plane of the trapping objective ($100\times/1.4$ oil, Plan Apo IR, Nikon, Tokyo, Japan). The beams are then collimated by a second objective ($60\times/1.2$ W, UPlanSApo, Olympus, Tokyo, Japan). Finally, a Glan-laser polarizer reflects one of the two beams, and lens (L5) images the back focal plane of the second objective on a position sensitive detector (Pacific Silicon Sensor, Westlake Village, CA). A part of the optical path is also used to image the beads on a charge coupled device camera. In order to avoid fluctuations from air currents, the optical path is fully enclosed. Most mechanical parts are custom designed to reduce drift and vibration.

IV. ROTATION OF POLARIZATION IN DOUBLE OPTICAL TWEEZERS USING A SINGLE LASER SOURCE

Force measurements in optical tweezers generally use either laser light going through the trapped particle for interferometric position detection or white light illumination for video based detection.[11] We use back focal plane interferometry to measure the force.[7] The method consists in evaluating the pattern of laser light diffracted by one of the trapped beads in the back focal plane of the condenser (or second objective) by imaging the pattern on a four-quadrant photodiode or a position sensitive detector.

As the two beams entering the trapping objective are of perpendicular polarization, if one wants to separately detect the position of one of the beads in its trap, one has to split by polarization the beams used to trap. Since a linearly polarized beam suffers from a nonhomogeneous rotation of polarization when going through a microscope objective, the discrimination of the two beams according to polarization cannot be perfectly achieved. If the polarization of one beam is checked after the back focal plane of the second objective with the polarizer, we observe that the transmitted light pattern exhibiting a polarization perpendicular to the incident beam is cross shaped (Fig. 3), in agreement with the calculation presented in Fig. 1(b). Consequently, the rotation of polarization allows for interference between the two beams, and the crosstalk that occurs is not simply the sum of the signals coming from the two beams separately. To understand the interference pattern appearing in the back focal plane of the second objective, we use the model introduced in Sec. II. For the sake of simplicity, we restrict the theoretical study to the case where no bead is trapped.

A. Model of interference without beads

To describe the interference pattern, we need to know the amplitudes and phases of the two beams in the detector plane. For this purpose we now closely consider the micro-
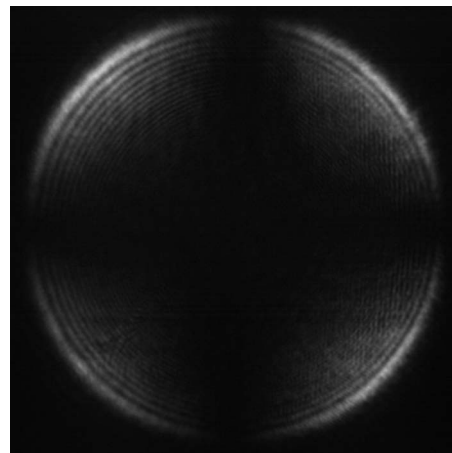

FIG. 3. Light remaining on the back focal plane of the second objective when a polarizer is used to reject the maximum of intensity arising from a single polarized beam after transmission through the microscope.

scope and detection part of the setup (Fig. 4) and, in particular, the image planes (A1), (A2), (B), (C), and (D).

The back focal plane (C) of the second objective is conjugated with the detector plane (D). The back focal planes of the two objectives (B) and (C) are also conjugated, and finally lenses (L3) and (L4) conjugate the back focal plane of the trapping objective, with plane (A1) centered on the mirror mounted on the piezoelectric stage for the first beam (directed by x' and y' axes) and with the equally distant plane (A2) on the other path for the second beam. Planes (A1) and (A2) are consequently conjugated with plane (D).

When the traps overlap, the beams enter the microscope with exactly the same angle. The phase shift $\Delta\phi_{(A)}$ between the phases of planes (A1) and (A2) (respectively, $\phi_{(A1)}$ and $\phi_{(A2)}$) is constant on plane (A1), so that $\Delta\phi_{(A)}=\phi_{(A1)}-\phi_{(A2)}=\phi_0$. This phase shift depends on the relative length of the optical paths of the two beams and is difficult to avoid because it corresponds to subwavelength (i.e., submicrometer) displacements of the optical components and is therefore particularly sensitive to thermal drift. To separate the two traps, one has to tilt the mirror mounted on the piezoelectric stage by an angle θ around the y' axis. If the rotation axis is centered on the optical path and if $\theta\ll1$, the corresponding phase shift takes the simple form
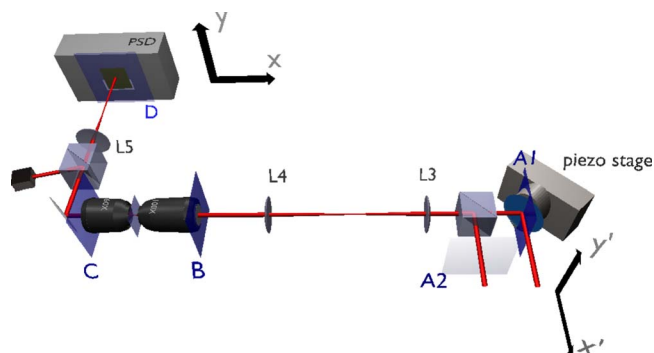

FIG. 4. (Color online) Schematic layout of the microscope and detection part of the setup. Planes (A1), (A2), (B), (C), and (D) are the ones described in the text.
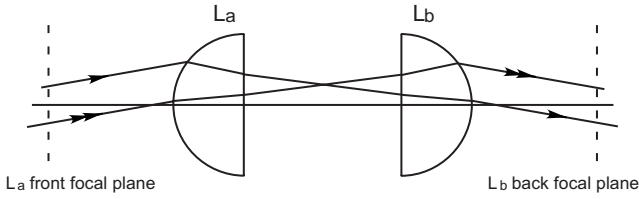
FIG. 5. Ray propagation through the two lens system. The two rays have symmetrical paths, but their rotations of polarization are different as described in the text.

$$\Delta\phi_{(A)}(x',\theta) = \phi_0 + \frac{4\pi}{\lambda}\theta x',$$

where λ is the light wavelength (see the Appendix for the calculation of this phase shift). Assuming that the magnification between planes (A1) and (A2) and the detector plane (D) is α, the phase shift between the two beams in plane (D) is given by

$$\Delta\phi_{(D)}(x,\theta) = \phi_0 + \frac{4\pi}{\lambda\alpha}\theta x.$$

The amplitude and phase of light going through two real microscope objectives may be difficult to calculate and requires knowledge of curvature, material, and coating of each element. The field symmetry should nevertheless be identical to the simpler case studied in Sec. II. Thus we use the model of Sec. II to describe the field amplitudes of the two beams on plane (D) and to evaluate the components that are transmitted by the polarizer.

As the phase shift between the two beams and their respective field amplitudes are given, we can describe the interference pattern occurring on the detector plane. We consider the specific and most useful case in which the polarizer after the second objective is rotated to reject the maximum of light coming from the moving trap. The vectors $\boldsymbol{\mathcal{E}}_1 = \mathbf{E}_1 e^{i\omega t}$ and $\boldsymbol{\mathcal{E}}_2 = \mathbf{E}_2 e^{i\omega t}$ denote the electric fields in the detector plane of the light coming from the fixed and mobile traps, respectively. The light intensity $I = \epsilon_0 c \langle |\boldsymbol{\mathcal{E}}_1 + \boldsymbol{\mathcal{E}}_2|^2 \rangle$ (Ref. 12) on the detector is given by

$$I(x,y,\theta) = \epsilon_0 c (|\mathbf{E}_1(x,y,\theta)|^2 + |\mathbf{E}_2(x,y,\theta)|^2$$
$$+ 2\mathbf{E}_1(x,y,\theta)\cdot\mathbf{E}_2(x,y,\theta)\cos[\Delta\phi_{(D)}(x,\theta)]).\quad (1)$$

The sum of the first two terms of Eq. (1) describes roughly the amplitude of a Gaussian beam, and we rewrite it as

$$\epsilon_0 c(|\mathbf{E}_1(x,y,\theta)|^2 + |\mathbf{E}_2(x,y,\theta)|^2) = \mathcal{A}(x,y,\theta).$$

If the optical components are perfectly centered and the two Gaussian beams impinge on the center of the back focal plane of the trapping objective, the symmetry of the system implies that $\mathcal{A}(x,y,\theta) = \mathcal{A}(x,-y,\theta)$. However, when $\theta \neq 0$, the rotation of polarization on the mobile trap is no more symmetrical regarding the $x>0$ and $x<0$ halves. As shown in Fig. 5, when the beam is refracted from air to the spherical interface of (L_a), the upper ray is refracted by a wider angle than the lower one. When the beam is refracted from the spherical interface of (L_b) to air, what used to be the upper ray of the beam is now refracted by a smaller angle than
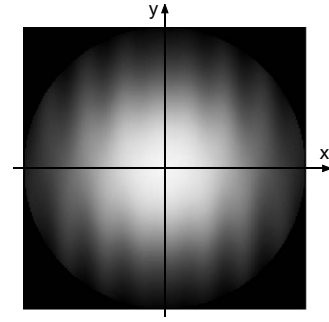

FIG. 6. Calculated interference pattern in the back focal plane of the second objective (the contrast is artificially enhanced for visualization). The two interfering beams exhibit perpendicular polarization before entering the microscope, and a polarizer is used to remove one of the two beams. The angular difference between the two beams is 1 mrad and NA=0.47.

what used to be the lower one. Because Fresnel coefficients differ when light is refracted from air to glass and glass to air, even if the paths of the two rays are symmetrical, the rotation of polarization that the two rays endure is not identical after passing through the two lenses. As a result, except for a few points, $\mathcal{A}(x,y,\theta) \neq \mathcal{A}(-x,y,\theta)$.

The last term of Eq. (1) creates interference, and we rewrite it as

$$2\epsilon_0 c\mathbf{E}_1(x,y,\theta)\cdot\mathbf{E}_2(x,y,\theta)\cos[\Delta\phi_{(D)}(x,\theta)] = \mathcal{B}(x,y,\theta).$$

Once more, if the alignment is perfect, the symmetry of the system implies that $\mathcal{B}(x,y,\theta) = -\mathcal{B}(x,-y,\theta)$. On the other hand, because the refraction is asymmetrical, as described above, except for a few special points, $\mathcal{B}(x,y,\theta) \neq \mathcal{B}(-x,y,\theta)$.

The illumination calculated assuming perfect alignment is shown in Fig. 6. The fringes are parallel to the y axis, and in each quarter, the distance between neighboring maxima equals $\alpha\lambda/2\theta$. The contrast of the fringes increases with the absolute rotation of polarization, and contrast inversion appears when going from left to right and from top to bottom due to the relative direction of the electric fields.

To calculate the expected normalized output signal of the position sensitive detector, we subtract the illumination on the $x>0$ half by the one on the $x<0$ half and divide this difference by the total illumination. When we increase the angle between the two beams, the system symmetries imply that the fringes have no effect on the detector signal; only the asymmetric refraction leads to a linear dependence of the signal on the angular position (for 2.5 mrad, the normalized difference reaches -5×10^{-6}).

In practice, the beams can be aligned to a precision of a few micrometers. To illustrate the consequence of this limitation, we now consider the case where one of the two beams is slightly translated from its centered position. As a typical example, if the beam creating the fixed trap is translated by 5 μm along the y axis in the back focal plane of the trapping objective, the image on the detector plane still looks close to the perfectly aligned case. The signal coming out of the detector is however very different (Fig. 7). The magnitude of the parasitic signal is higher, increases with the translation of the beam (data not shown), and shows a dependence on the phase shift ϕ_0. The variation of the signal when the traps
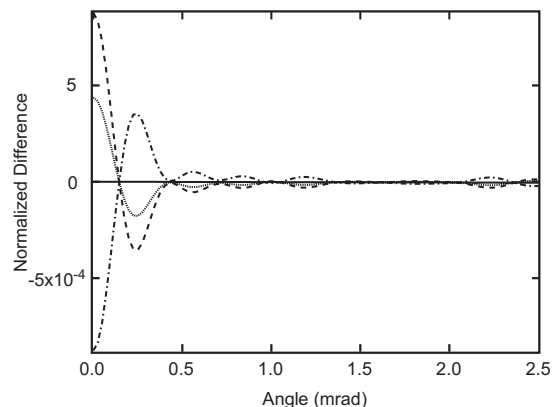
FIG. 7. Theoretically expected normalized output signal of a position sensitive detector in the presence of the two beams when the mobile beam is deflected and NA=0.47. The fixed trap is translated by +5 μm along the y axis in the detector plane (D). The phase differences ϕ_0 between the two beams are 0 (dashed), $\pi/3$ (dotted), $\pi/2$ (solid), and π (dash-dotted).

move apart is closely linked to the appearance of new fringes on the detector plane. As a result, the parasitic signal takes a complicated form, depending on misalignments and NAs.

B. Crosstalk in force measurements with beads

In order to evaluate the crosstalk occurring during a force measurement, we trap two 0.97 μm silica beads (Bangs Laboratories Inc., Fishers, IN) in the two tweezers; one bead is fixed and the other one is moved apart such as in a single molecule experiment. The force is measured on the bead in the fixed trap. Force is calibrated by measuring the power spectrum of the Brownian motion of a trapped bead with a spectrum analyzer.[13] Exciting separately the mobile or the fixed trap and selecting the corresponding polarization in the detection path, we measured the stiffness of each trap of the double tweezers. The difference between these two stiffnesses is below 5%, an uncertainty comparable to the one caused by common bead to bead variation. A typical experimental interference pattern occurring in the detector plane is presented in Fig. 8. When the two beads are separated by a few micrometers in the sample (4 μm in Fig. 8), the ob-
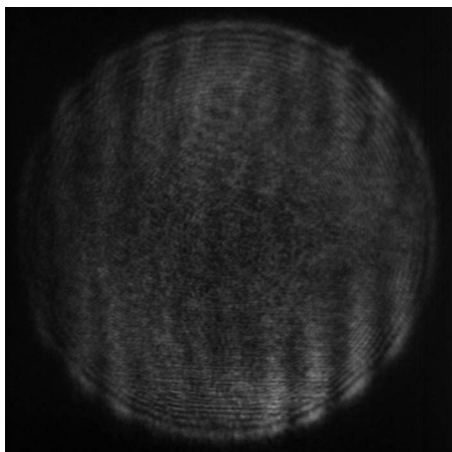

FIG. 8. Interference pattern seen in the back focal plane of the second objective with two silica beads trapped. The two beads each exhibit a diameter of 0.97 μm and are separated by 4 μm in the sample plane.
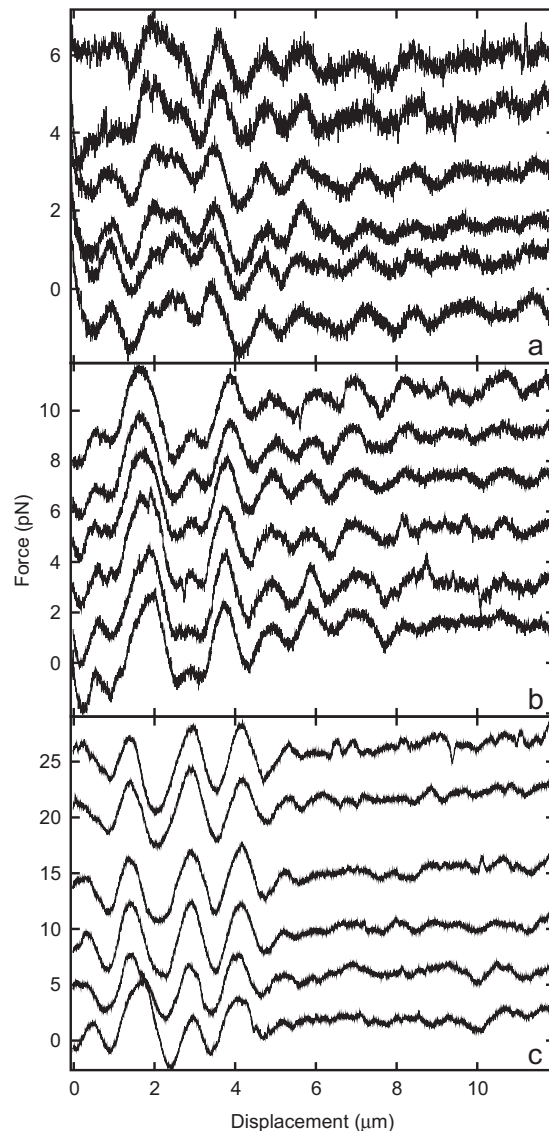

FIG. 9. Dependence of the parasitic signal on the stiffness and the separation between the two traps. The force is measured on the fixed trap using two unlinked beads. The stiffness k_f of the fixed trap and the total laser power in the back focal plane of the trapping objective P are (a) $k_f=192$ pN/μm and $P=800$ mW, (b) $k_f=339$ pN/μm and $P=1.40$ W, and (c) $k_f=593$ pN/μm and $P=2.05$ W. The displacement velocity between the two traps is 1 μm/s, and sampling is done at 800 Hz with an antialias filter of 352 Hz. Individual curves are vertically shifted for clarity [1.5 pN between subsequent curves in (a), 2 pN in (b), and 4 pN in (c)]. Notice the change in vertical axis scaling between (a), (b), and (c).

served light pattern exhibits the characteristics described in Sec. IV A. Force measurements resulting from the evaluation of the light pattern on a position sensitive detector are done at different laser powers; we measure a few curves for each power to illustrate the effect of drift on the signal [Fig. 9(a)–9(c)]. The interference pattern creates a parasitic signal whose magnitude decreases when the distance between the beads increases and is approximately proportional to laser power. Actually, when the back focal plane method is used to measure force, one easily finds that force is proportional to the difference of illumination on the two detector halves. Consequently, the output voltage of the detector is commonly proportional to the force regardless of laser power, while a given interference pattern generates a signal propor-
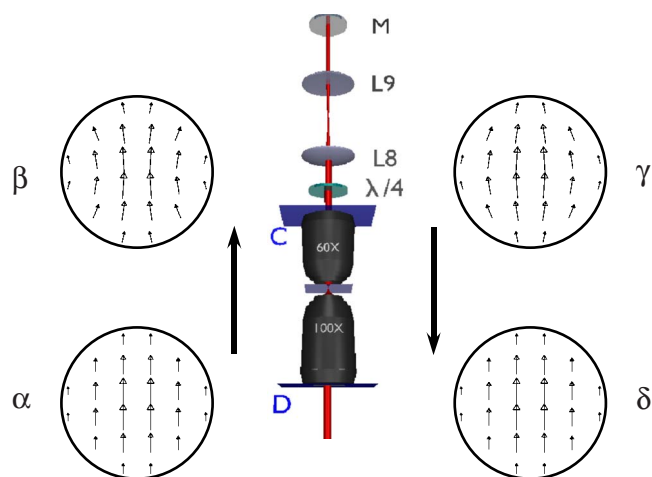
FIG. 10. (Color online) Schematic layout of our polarization rectifier. The electric fields are given for the first passage through the microscope in the back focal plane of the first objective (α) and in the back focal plane of the second objective (β). For the second passage, they are given in the back focal plane of the second objective (γ) and the back focal plane of the first objective (δ).

tional to the laser power. The pattern of the signal is difficult to reproduce because it depends on alignments and is subject to drift.

Setup alignments are an important issue that should be considered carefully. First, to ensure that the number of fringes is equal for $x>0$ and $x<0$, the phase shift between the two beams must be adjusted. One way to adjust the phase is to add a parallel glass slide in the path of one of the beams before they are combined. A rotation of the glass slide will add a phase for this beam until the number of fringes is exactly the same for both detector halves. This rotation also adds a small translation of the beam, but it is possible to keep the translation small enough to not increase significantly the parasitic signal. Second, the image of the center of rotation of the mirror mounted on the piezoelectric stage has to be exactly in the center of the detector to assure the symmetry of the pattern when rotating the mirror. Finally, as it has already been pointed out in the previous paragraph, the beams should be centered on the back focal planes of both objectives, and the back focal plane of the second objective should be centered on the detector.

V. HOW TO DECREASE CROSSTALK

A. Polarization rectification

As the interference originates from the rotation of polarization in the microscope, an obvious way to reduce crosstalk is to reduce the rotation. One fully optical method was first developed by Inoué to increase contrast in polarizing microscopy.[9] His idea was to compensate rotation by a combination of a half-wave plate and spherical surfaces such as glass or air meniscus, which he called "the polarization rectifier."

We investigate a new method based on the same idea, but one that is easier to implement with optical tweezers. It consists in going through the microscope twice and compensating rotation of polarization by a quarter-wave plate. A schematic layout is given in Fig. 10.

Let us consider a linearly polarized Gaussian beam entering the system (α). When it passes the two objectives for the first time, the electric field endures a first transformation due to the rotation of polarization (β). The beam is reflected in the upper part of the rectifier and passes twice through the quarter-wave plate. This adds twice the opposite initial rotation (γ). Finally, when the beam goes through the microscope for the second time, it again endures the initial transformation (δ). As the electric field is rotated twice by the same angle and once by the double opposite angle, the electric field going out of the polarization rectifier is theoretically perfectly linearly polarized. It remains to detect the bead position by back focal plane interferometry, requiring to image the light pattern of the back focal plane of the second objective (β) with a corrected polarization. The combination of lenses (L8) and (L9) and the mirror (M) enables us to image plane (C) on itself, and as planes (C) and (D) are conjugated, the light pattern used for detection (β) is finally seen on plane (D). As the polarization is corrected with the rectifier, the light pattern on plane (D) is appropriate for back focal plane interferometry.

However, some critical points have to be mentioned. First, by going back in the microscope, the beams create replicated tweezers that should not perturb the trapping ones. In our configuration it is possible to align the beams going first in the microscope on the optical axis, and then to tilt as less as possible the mirror (M) so that replicated tweezers are far enough to not disturb the trapping tweezers. Second, when the beams are entering the microscope for the first time, a significant part of the light is reflected on surfaces, especially by the glass water interfaces. This generates reflected beams that may be difficult to separate from the ones we want to detect. Third, as the beams are trapping beads only when they first go through the microscope, but not when they go back, paths are different in the two directions. Finally, because Fresnel coefficients are different when light is refracted from glass to air and air to glass interfaces, the rotation of polarization is different when a beam passes through an objective with opposite directions on the same path. As a result, the rotation of polarization may be the same when going through the microscope with opposite directions only if the trapping objective and the condenser are identical. As this is not the case in our experiments, the transformation may not be perfectly achieved.

Using the trapping objective described above and a high NA oil immersed objective as a collimation objective (100$\times$/1.3 oil, EC Plan-NeoFluar, Carl Zeiss, Thornwood, NY), this method permits us to decrease crosstalk by a factor of 4. The power ratio of the two perpendicularly polarized beams measured with the Glan-laser polarizer is 4×10^{-3} without the rectifier and 1×10^{-3} when it is used at N.A.=1.3. The method appears to be better suited when high NA is used. An improvement of less than 2 is found at NA lower than 0.9.

B. Frequency shift of one beam

The second method to reduce the crosstalk coming from interference is to shift the frequency of one of the two beams. In our apparatus, the beam of the mobile trap goes through an acousto-optic frequency shifter (AA Optoelectronic, Or-
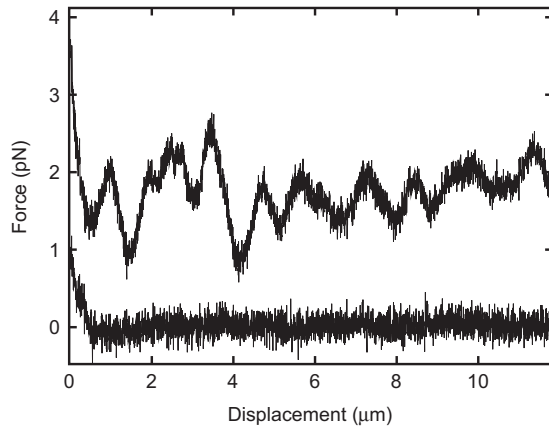
FIG. 11. Force measurements with two 0.97 μm silica beads trapped with the frequency shifter on (bottom: $k_f=213$ pN/μm and $P=910$ mW) and off (top: $k_f=192$ pN/μm and $P=800$ mW). The displacement velocity between the two beads is 1 μm/s, and sampling is done at 800 Hz with an antialias filter of 352 Hz. The signal measured without the frequency shifter on is shifted vertically for better visualization.

say, France) before being deflected by the piezoelectric tilt stage. In this way, as one retrieves the first order of the acousto-optic device, the beam coming from the mobile trap is shifted by the acoustic frequency f_0 of the shifter, in our case 80 MHz.

The intensity on the detector plane is now

$$I(x,y,\theta) = \epsilon_0 c(|\mathbf{E}_1(x,y,\theta)|^2 + |\mathbf{E}_2(x,y,\theta)|^2$$
$$+ 2\mathbf{E}_1(x,y,\theta) \cdot \mathbf{E}_2(x,y,\theta)$$
$$\times \cos[2\pi f_0 t + \Delta\phi_{(D)}(x,\theta)]).$$

As the electronics of the position sensitive detector has a bandwidth of about 100 kHz, it acts as a low pass filter for higher frequencies; the signal coming from the rapidly moving fringes is therefore rejected, and crosstalk coming from the interference pattern is no more measurable. Figure 11 provides an example of force measurements done with and without the frequency shifter. The signal measured with the frequency shifter shows no dependence on the bead separation, except for the first 600 nm where the proximity of the beads affects detection.

While frequency shifting indeed enables us to average out interference effects, one should remember that the rotation of polarization still occurs and two beams are seen on the detector plane. We did the following experiment to estimate the influence of the mobile trap on the detection of force in the fixed trap. The conversion coefficient, which relates force to the output voltage of the detector, was determined by measuring the power spectrum of the Brownian motion of one 0.97 μm silica bead in its trap. This measurement was done separately for the two traps (the other trap was switched off during the measurement). The laser light from the mobile trap was reflected with the polarizer. From these measurements we estimated that the conversion coefficient for the fixed trap was 0.26 V/pN and 5.4 $\times 10^{-3}$ V/pN for the mobile trap, meaning that about 2% of the force applied on the bead in the moving trap is detected on the fixed trap. This effect should be considered when an accurate measurement of the absolute value of the force
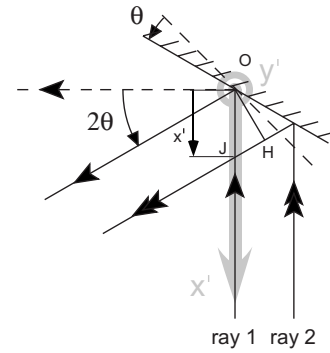

FIG. 12. Geometrical parameters describing the deflection of the mobile trap by the piezoelectric mirror mount.

measurement is needed. In contrast to the interference effect, this direct crosstalk does not depend on laser power.

VI. CONCLUSIONS

The rotation of polarization in double optical tweezers creates parasitic signals that should be taken care of, especially for applications that require high trap stiffness or high laser power. Indeed, whereas the output voltage of the detector is commonly proportional to the force regardless of laser power, a given interference pattern generates a signal proportional to the laser power. Consequently, an important feature of this phenomena is that it is usually seen when laser power is high (i.e., 0.5 W or higher). For a low power trapping laser, parasitic signal still exists but may be hidden by noise.

The rectification of polarization enables us to decrease the crosstalk between the two traps, but not to annihilate it. We found that an even simpler and most effective method is to shift the frequency of one of the two beams. Even if crosstalk between the two traps is still occurring, it is small enough for most applications.

ACKNOWLEDGMENTS

APPENDIX: GEOMETRICAL DEFINITIONS AND PHASE SHIFT CALCULATION

We give here a definition of the geometrical parameters used in Sec. IV (Fig. 12) and calculate the phase shift $\Delta\phi_{(A)}$. As explained before, when the two beams have the same direction (i.e., $\theta=0$), the phases on planes (A1) and (A2) are constant, so that the phase shift between the two beams is also constant and equals ϕ_0 [the planes (A1) and (A2) are indicated in Fig. 4]. Let us now consider the case where the mobile beam is deflected by the piezoelectric stage. As defined earlier, plane (A1) is directed by the x' and y' axes, and we suppose that $\theta \ll 1$. Because the beam is parallel, its phase is constant on any plane perpendicular to its direction of propagation, and in particular its phase is constant on segment [OH]. As O is on the rotation axis of the mirror, the phase of ray 1 reflecting on O is constant on plane (A1) with the deflection of the beam. In comparison to ray 1, ray 2 passing on point J, of abscissa x', has the additional path [HJ]$=2\theta x'$ before hitting plane (A1), so that its phase is

$\phi_{(A1)}(x', \theta) = \phi_{(A1)}(0, \theta) + (2\pi/\lambda)2\theta x'$. Finally, as the phase on plane (A2) is still constant, the phase shift between planes (A1) and (A2) is

$$\Delta\phi_A(x', \theta) = \phi_0 + \frac{4\pi}{\lambda}\theta x'.$$

[1] A. Ashkin, J. M. Dziedzic, and T. Yamane, Nature (London) **330**, 769 (1987).

[2] W. J. Greenleaf, M. T. Woodside, E. A. Abbondanzieri, and S. M. Block, Phys. Rev. Lett. **95**, 208102 (2005).

[3] P. Mangeol, D. Côte, T. Bizebard, O. Legrand, and U. Bockelmann, Eur. Phys. J. E **19**, 311 (2006).

[4] J. W. Shaevitz, E. A. Abbondanzieri, R. Landick, and S. M. Block, Nature (London) **426**, 684 (2003).

[5] E. A. Abbondanzieri, W. J. Greenleaf, J. W. Shaevitz, R. Landick, and S. M. Block, Nature (London) **438**, 460 (2005).

[6] J. R. Moffitt, Y. R. Chemla, D. Izhaky, and C. Bustamante, Proc. Natl. Acad. Sci. U.S.A. **103**, 9006 (2006).

[7] F. Gittes and C. F. Schmidt, Opt. Lett. **23**, 7 (1998).

[8] S. Inoué, Exp. Cell Res. **3**, 199 (1952).

[9] S. Inoué and W. L. Hyde, J. Biophys. Biochem. Cytol. **3**, 831 (1957).

[10] M. Shribak, S. Inoué, and R. Oldenbourg, Opt. Eng. (Bellingham) **41**, 943 (2002).

[11] K. C. Neuman and S. M. Block, Rev. Sci. Instrum. **75**, 2787 (2004).

[12] E. Hecht, *Optics*, 2nd ed. (Addison-Wesley, Reading, MA, 1987).

[13] U. Bockelmann, P. Thomen, B. Essevaz-Roulet, V. Viasnoff, and F. Heslot, Biophys. J. **82**, 1537 (2002).